Synergistic Effects of Fumed Silica on Intumescent Flame-Retardant Polypropylene

Lei Ye, Qianghua Wu, Baojun Qu

CAS Key Laboratory of Soft Matter Chemistry, Department of Polymer Science and Engineering, University of Science and Technology of China, Hefei, Anhui 230026, China

ABSTRACT: The synergistic effects of fumed silica on the thermal and flame-retardant properties of intumescent flame retardant (IFR) polypropylene based on the NP phosphorus-nitrogen compound have been studied by Fourier transfer infrared (FTIR) spectroscopy, cone calorimeter test (CCT), scanning electron microscopy (SEM), thermogravimetric analysis (TGA), limiting oxygen index (LOI), and UL-94 tests. The LOI and UL-94 data show that when ≤1 wt % fumed silica substituted for the IFR additive NP can increase 2 to 4% LOI values of the PP blends and keep the V-0 rating. The data obtained from the CCT tests indicate the heat release rates (HRR) reduce by about 23% for the PP/NP sample with 0.5 wt % fumed silica, whereas the mass loss rates (MLR) and total heat release (THR) values are much lower than those of the PP/NP samples without fume silica. The TGA data demonstrate that a suitable amount of fumed silica can increase the thermal stability and charred residue of the PP/IFR/SiO$_2$ blends after 500°C.

The morphological structures of charred residues observed by SEM give positive evidence that a suitable amount of fumed silica can promote the formation of compact intumescent charred layers and prevent the charred layers from cracking, which effectively protects the underlying polymer from burning. The dynamic FTIR spectra reveal that the synergistic flame-retardant mechanism of a suitable amount of fumed silica with IFR additive is due to its physical process in the condensed phases. However, a high loading of fumed silica restricts the formation of charred layers with P—O—P and P—O—C complexes formed from burning of polymer materials and destroys the swelling behavior of intumescent charred layers, which deteriorates the flame retardant and thermal properties of the PP/IFR blends. © 2009 Wiley Periodicals, Inc. J Appl Polym Sci 115: 3508–3515, 2010

Key words: polypropylene; fumed silica; synergistic effect; intumescent; flame retardant

INTRODUCTION

Polypropylene is used extensively for many applications, such as building materials, furniture, automobiles, and so on. However, its usage is often limited for its poor flame resistance. Traditionally, the halogen-containing compounds, alone or in conjunction with antimony trioxide, are the main flame retardants of PP,[1] but halogen-containing flame-retarded PP systems may produce large amounts of smoke and toxic gas on burning that can choke people exposed to the toxic and acidic fumes and can damage costly equipment.

As halogen-free flame-retardant products, intumescent flame retardants (IFR) containing phosphate and nitrogen are expected to be used in PP. An intumescent flame-retardant system is usually composed of three components: an acid source, a char-forming agent, and a blowing agent.[2,3] The proposed mechanism of intumescent retardant materials is the foamed cellular charred layers formed on heating

acting as a physical barrier on the surface, which slow down heat and mass transfer between the gas and condensed phase and protect the underlying materials from heat flux or flame. According to the studies in our laboratory,[4–6] the phosphorus-nitrogen compound NP is an excellent IFR additive that performs as a acid source, a carbonizing compound, and a blowing agent in polyolefins, especially in PP. To enhance the flame retardancy, some synergistic agents have been used in IFR systems, such as zeolites,[7] some transitional metal oxides, and metal compounds.[6,8,9] Many researchers have shown that synergistic agents can efficiently increase the strength and stability of charred layers and promote the catalyzing reactions in the PP/IFR blends.

Fumed silica is usually used as an enhancing agent in thermoplastic polymers to increase the mechanical properties, such as tensile strength and toughness. Kashiwagi and coworkers have reported the flame-retardant behavior of silica in polypropylene blends.[10] The effect of fumed silica on the ethylene-vinyl acetate/magnesium hydroxide blends has been reported recently.[11] However, as far as we are aware, no work has been done on the synergistic effect of fumed silica in PP/IFR blends.

This work is mainly devoted to investigating the synergistic effect of fumed silica with NP on combustion and flame-retardant properties of the PP/IFR blends by cone calorimeter test (CCT), scanning electron microscopy (SEM), Fourier transfer infrared (FTIR) spectroscopy, thermogravimetric analysis (TGA), limiting oxygen index (LOI), and UL-94 tests.

EXPERIMENTAL

Materials

Commercial polypropylene (PP F401), from Yangzi Oil Company with a melt index of 2.0 g/min (230°C/2.16 kg) was used as a matrix (Nanjing, China). Fumed silica (SiO_2) with a specific surface area of 150 m^2/g and an average particle size of 14 nm was obtained from Degussa (Essen, Germany). The phosphorus-nitrogen compound NP containing 15.6 wt % P, 27.5 wt % N, with a particle size of 400 mesh from Zhuhai Deco Chemical Reagent Corporation (Zhuhai, China) were used as FR additives.

All the above chemicals are commercial products used as received.

Sample preparation

All the samples were mixed for 10 min at 180°C in a Rheomixer XSS-300 (made in Shanghai). After mixing, the samples were hot-pressed under 10 MPa for 5 min at 180°C into sheets of suitable thickness. Sheets size and thickness were dependent on the testing methods used in the present study.

The $PP/NP/SiO_2$ samples with a given amount of PP, NP, and SiO_2 are marked as PP/NP-m/SiO_2-n, where m and n indicate the weight percent of NP and SiO_2 in the $PP/NP/SiO_2$ blends, respectively. For example, the PP/NP-23/SiO_2-2 sample indicates the weight percent of 23 NP, 2 SiO_2, and 75 PP.

Measurements

The cone calorimeter tests were carried out using a Redcroft Cone Calorimeter, following the procedure defined in ISO 5660 on 4-mm-thick 100 × 100 mm^2 plaques. Each specimen was wrapped in aluminium and exposed horizontally to an external heat flux of 35 kW/m^2. Various parameters can be measured, including time to ignition (TTI), heat release rate (HRR) as a function of time, peak of heat release rate (pk-HRR), mass loss rate (MLR), and total heat release (THR). The experimental error of data from the cone calorimeter was about 5%.

The SEM of the char layers were analyzed by a JEOL JSM-6700F Field emission scanning electron microscope. The specimens were previously coated with a conductive layer of gold.

TABLE I
LOI and UL-94 Data of PP/NP Blends with Different NP Loading Levels

Samples	PP (wt %)	NP (wt %)	LOI	UL-94
1	80	20	31	Fail
2	79	21	31.5	Fail
3	78	22	32	V-1
4	77	23	32.5	V-0
5	76	24	33	V-0
6	75	25	34	V-0

TGA was performed on a Shimadzu TGA-50H thermoanalyzer at a scan rate of 10°C/min under the air flow rate of 2 × 10^{-5} m^3/min.

The dynamic FTIR spectra were recorded with a MAGNA-IR 750 spectrometer (Nicolet Instrument). The data were measured using the KBr disk method with a heating rate of 5°C/min. The FTIR software was used to measure peak intensity of the FTIR spectrum to compare the degradation rate of materials, the formation of rates, and relative concentration of thermal oxidation products. The relative concentration can be calculated by the relative intensity ratio of related peak height to the peak height at 1375 cm^{-1} at room temperature. Repeated experiments showed that there was no real difference for a small change of sample thickness in measuring the relative peak intensity.

LOI measurements were carried out using a HC-2 type instrument (made in China) in accordance with ASTM D 2863-77. The samples used for the test were of dimensions 100 × 6.5 × 3 mm^3.

The UL-94 vertical test was carried out using a CZF-1 type instrument (made in China) on sheets of 127 × 12.7 × 3 mm^3 according to ASTM D 635-77.

RESULTS AND DISCUSSION

Effect of fumed silica on the LOI and UL-94 values of PP/IFR blends

The LOI and U-94 data of PP with different contents of IFR additive NP are listed in Table I. It can be seen that the flame retardancy of the PP/IFR composites without fume silica was quite high, and the LOI value reached 32.5% and passed the UL-94 V-0 rating when the content of NP is only 23 wt % in the PP/IFR blends because the NP is an excellent IFR additive that performs as a acid source, a carbonizing compound, and a blowing agent in polyolefins, especially in PP, as reported by our previous work.[4–6]

Figure 1 presents the changes of LOI values versus fumed silica levels for the $PP/NP/SiO_2$ blends at the total amount of 25 wt % additives kept constant. It can be seen that the LOI values of PP/NP blend without SiO_2 is 34%. The LOI values of $PP/NP/SiO_2$ blends increase to the maximum value 38% quickly
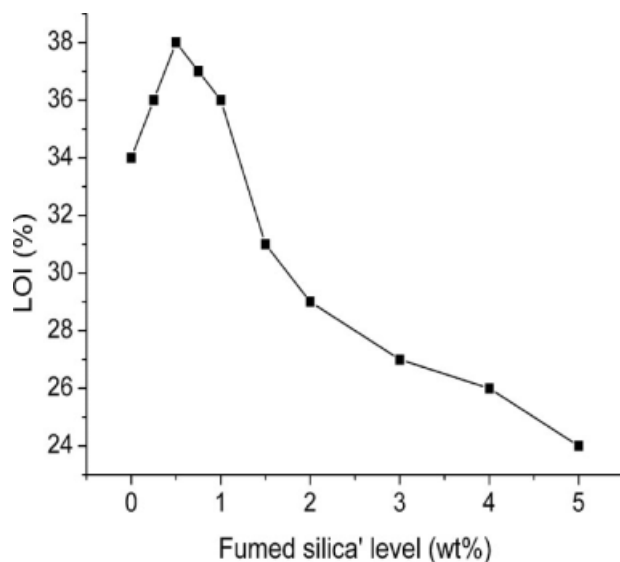
Figure 1 Changes of LOI values versus fumed silica level for the PP/NP/SiO$_2$ at the total amount of additives kept constant at 25 wt %.

when the loading of SiO$_2$ increases to 0.5 wt %. The corresponding LOI and UL-94 data are listed in Table II. It can be seen that ≤1 wt % SiO$_2$ can increase 2 to 4% LOI values and keep the UL-94 V-0 rating. However, the further increase of SiO$_2$ amount to >1 wt % leads to rapid decrease in the LOI values of PP/NP/SiO$_2$ samples. Their LOI values are 3 to 10% lower than 34% of the PP/NP-25 sample without SiO$_2$. The LOI values of PP/NP/SiO$_2$ samples with about 1.5 wt % SiO$_2$ have been decreased to 31%, whereas all these samples cannot pass the UL-94 V-0 rating.

Figure 2 shows the photographs of various charred PP/NP/SiO$_2$ samples obtained after the LOI test. It can be seen from Figure 2(A,B) that the char residues of the PP/NP-25 and PP/NP-24.5/SiO$_2$-0.5 samples show the features of large intumescent charred layers compared with those of the PP/NP-22/SiO$_2$-3 and PP/NP-20/SiO$_2$-5 samples in Figure 2(C,D), which indicates that they can more efficiently protect the underlying polymeric materials from further be burning.

The above results indicate that there is an optimum concentration on the synergistic effect of fumed silica with NP in the PP/NP/SiO$_2$ blends, and the high loading of fume silica will deteriorate the swelling behavior and formation of intumescent char layers of the PP/IFR blends.

Dynamic flammability characterization of PP/IFR/SiO$_2$ blends

The cone calorimeter test, based on the oxygen consumption principle, has been widely used to evaluate the flammability characteristics of materials because its results correlate well with those obtained from large-scale fire tests and can be used to predict the combustion behavior of materials in real fires.[12] For instance, the peak HRR is a very important parameter that can be used to express the intensity of fire.[13] Fire performance index (FPI) is defined as the ratio of TTI to pk-HRR, which is independent of the tested sample thickness and is often used to predict whether a material can easily develop drastic combustion after ignition.[14] Therefore, the greater the FPI value, the better is the fire resistance. Figure 3 presents the dynamic curves of HRR versus time for pure PP, PP/NP-25, and PP/NP-24.5/SiO$_2$-0.5 samples with the total loading of NP and SiO$_2$ kept constant at 25 wt %. Pure PP burns out within 400 s after ignition, as shown in Figure 3(A). A very sharp HRR peak of pure PP sample appears at the range of 150 to 200 s, with a peak heat release rate (pk-HRR) of 1025 kW/m^2. However, the PP/NP-25 and PP/NP-24.5/SiO$_2$-0.5 samples show significantly depressed HRR peaks and prolongation of the combustion times. The pk-HRR value for the PP/NP-24.5/SiO$_2$-0.5 samples are 124 kW/m^2, which is reduced by about 23% compared with the pk-HRR value of the PP/NP-25 sample (160 W/m^2). Before 100 s, the HRR curves of PP/NP-25 and PP/NP-24.5/SiO$_2$-0.5 samples exhibit a small, sharp peak, as shown in Figure 3(B). It has been assigned to the partial decomposition of phosphorus-nitrogen compound leading to some gas phase flame-retardant effect, as reported in the literature.[15] Table III lists the TTI, pk-HRR, and their ratio (FPI) values of pure PP, PP/NP-25, PP/NP-24.5/SiO$_2$-0.5, PP/NP-22/SiO$_2$-3, and PP/NP-22 samples. The TTI values of PP/NP-25 and PP/NP-24.5/SiO$_2$-0.5 samples are much lower than that of the pure PP. It can be seen from Table III that the PP/NP-24.5/SiO$_2$-0.5 sample has the greatest FPI value 0.2016 among the above samples, which indicates the PP/NP-24.5/SiO$_2$-0.5 sample has the best fire resistance. However, the PP/NP-22/SiO$_2$-3 sample shows the highest pk-HRR value and lowest TTI and FPI values among these flame-retardant samples, except for pure PP. These data indicate that a suitable amount of fumed silica

TABLE II
LOI and UL-94 Data of PP/NP/SiO$_2$ Blends with the Total Loading Level of Additives Kept Constant at 25 wt %

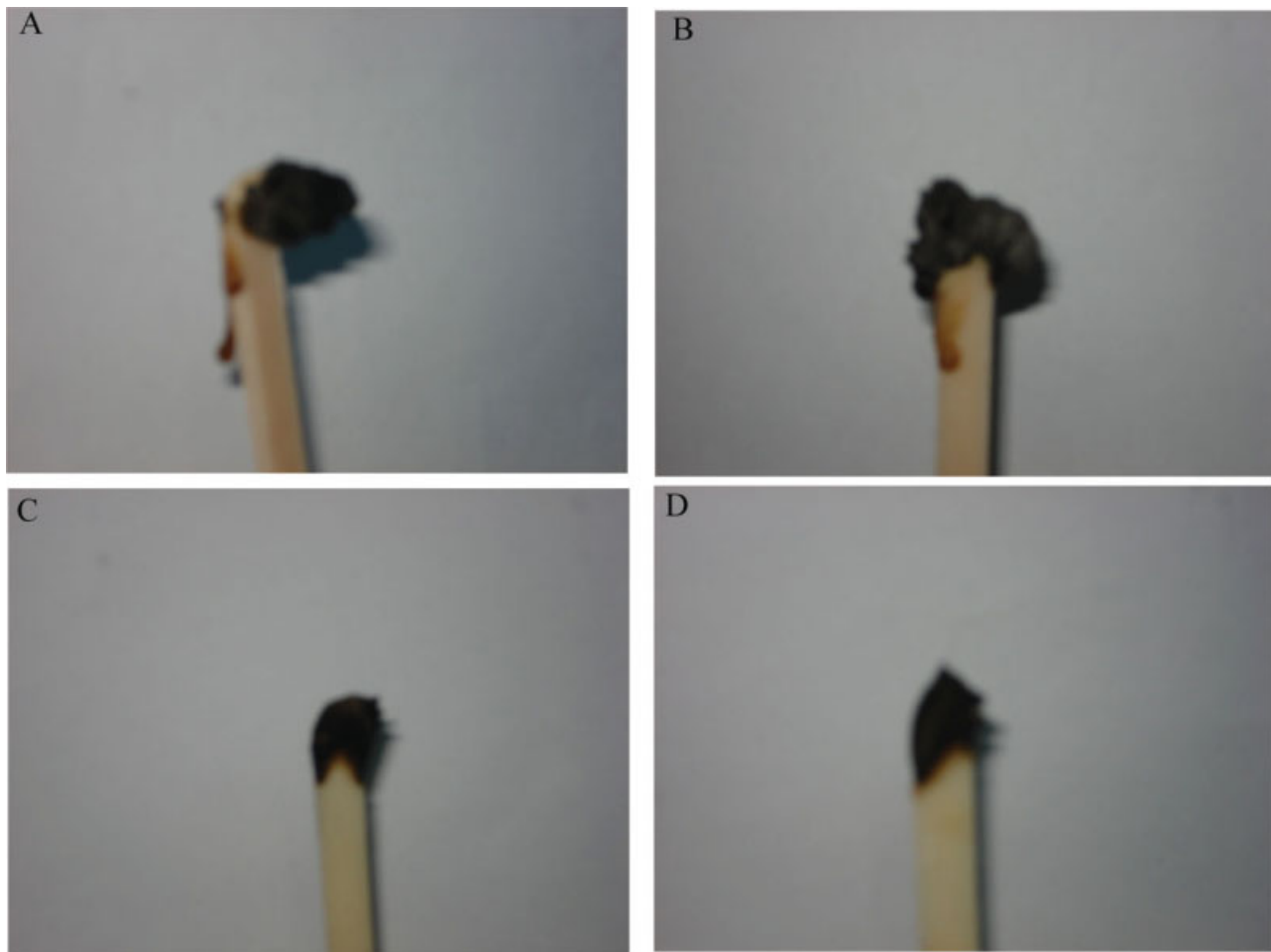| SiO$_2$ (wt %)	0	0.25	0.5	0.75	1.0	1.5	2.0	3.0	4.0	5.0
LOI	34	36	38	37	36	31	29	27	26	24
Ul-94	V-0	V-0	V-0	V-0	V-0	Fail	Fail	Fail	Fail	Fail

Figure 2 Photographs of the PP/NP/SiO$_2$ samples with different amount of SiO$_2$ after LOI test: (A) PP/NP-25; (B) PP/NP-24.5/SiO$_2$-0.5; (C) PP/NP-22/SiO$_2$-3; (D) PP/NP-20/SiO$_2$-5. [Color figure can be viewed in the online issue, which is available at www.interscience.wiley.com.]

has a synergistic effect of flame retardancy with NP in the PP/IFR blends, whereas the high loading of fume silica will deteriorate the flame-retardant properties of PP/IFR blends.

Figures 4 and 5 present the MLR and THR curves versus time for pure PP, PP/NP-25, and PP/NP-24.5/SiO$_2$-0.5 samples with the total loading of NP and SiO$_2$ additives kept constant at 25 wt %, respectively. It can be seen from Figure 4 that the MLR values of PP/NP-25 and PP/NP-24.5/SiO$_2$-0.5 samples significantly decrease compared with pure PP. The pk-MLR value of PP/NP-24.5/SiO$_2$-0.5 sample
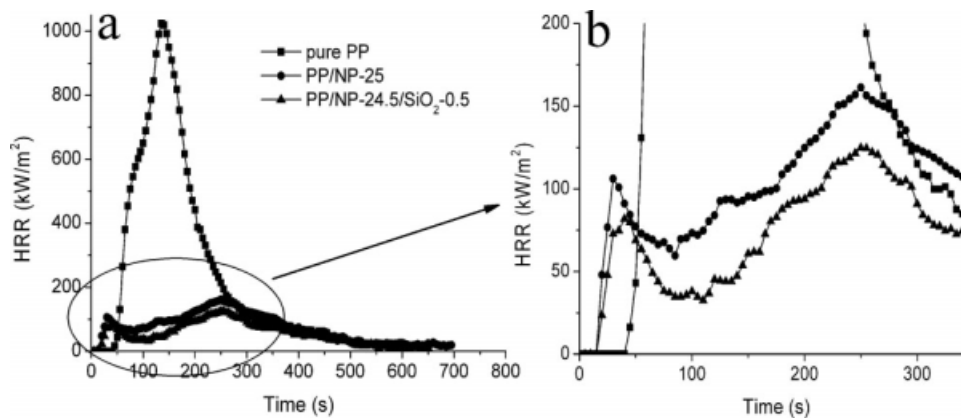

Figure 3 (A) Dynamic curves of HRR versus time for pure PP, PP/NP-25, and PP/NP-24.5/SiO$_2$-0.5 samples with the total loading of NP and SiO$_2$ kept constant at 25 wt %. (B) Magnification diagram at the range of 0 to 300 s.

TABLE III
Flammability Data of Pure PP, PP/NP, and PP/NP/SiO$_2$ Samples Determined from
Cone Calorimeter Tests

Samples	TTI (s)	pk-HRR (kW/m^2)	FPI (m^{2}s/kW)	pk-MLR [g/(s m^2)]	THR (MJ/m^2)
Pure PP	42	1025	0.041	0.143	137.7
PP/NP-25	21	160	0.131	0.029	49.1
PP/NP-24.5/SiO$_2$-0.5	25	124	0.202	0.023	35.1
PP/NP-22	22	170	0.129	0.031	50.3
PP/NP-22/SiO$_2$-3	17	341	0.050	0.069	87.9

is 0.023 g/(s m^2) lower than 0.029 g/(s m^2) of PP/NP-25 sample, which also indicated the synergistic effect of fumed silica with NP in PP/IFR blends. It can be seen from Figure 5 that the THR of pure PP sample is 137.7 MJ/m^2 and much higher than 49.1 and 35.1 MJ/m^2 for the PP/NP-25 and PP/NP-24.5/SiO$_2$-0.5 samples, respectively, at the end of combustion. The lower THR means a better flame-retardant property of blends. Table III lists the flammable data of various samples obtained from the cone calorimeter tests. The MLR and THR data from Table III give the positive evidence again that a suitable amount of fumed silica has a synergistic effect of flame retardancy with NP in the PP/IFR blends, and an excessive amount of fumed silica will deteriorate the flame-retardant properties of PP/IFR blends.

Thermogravimetric behaviors of PP/IFR/SiO$_2$ blends

Figure 6(A,B) presents the TGA and DTG curves of pure PP, PP/NP-25, and PP/NP/SiO$_2$ samples with different content of SiO$_2$, respectively. The pure PP shows one-step weight loss in the range of 280 to 450°C and leaves no residues after 450°C. The degradation of PP/NP-25 sample occurs in two steps. The

first step is an intumescent process that occurred at the temperature range of 200 to 400°C and lost approximately 70 to 80% mass loss. The second step occurred at the range of 400 to 700°C and can be assigned to the thermal oxidation degradation of the intumescent char structures. It can be observed from Figure 6(A) that the onset decomposition temperatures of the PP/IFR samples are much lower than that of pure PP. This is because NP is easy to decompose and to form phosphorus or phosphoric acid and release nitrogen gas, which is beneficial to promote the formation of cross-linking structures and ultimately carbonization on the surface of the polymer. With the increase of temperature, more intumescent carbonaceous materials were formed and thus enhanced the thermal stability of the polymic materials.[15] And it can be seen from Figure 6(A) that the PP/NP-24.5/SiO$_2$-0.5 sample shows higher thermal decomposition temperature than the PP/NP-25 sample at the range of 200 to 700°C and leaves more residues after 500°C. However, the PP/NP-22/SiO$_2$-3 sample with 3 wt % fumed silica shows much lower thermal decomposition temperature after 150°C and much lower residues than the PP/NP-25 and PP/NP-24.5/SiO$_2$-0.5 samples. For example, when 50% weight loss was selected as a
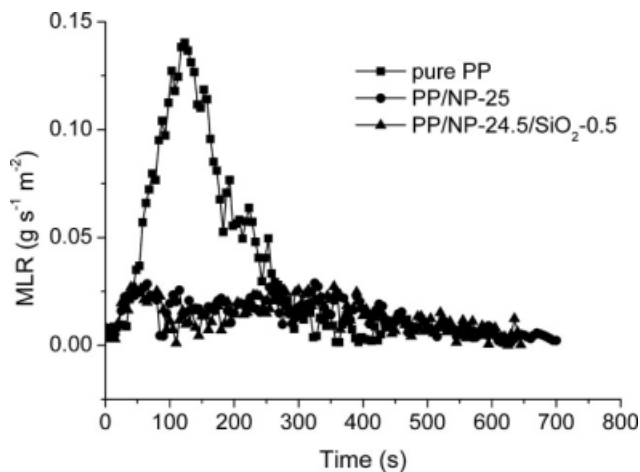

Figure 4 Dynamic curves of MLR versus time for pure PP, PP/NP-25, and PP/NP-24.5/SiO$_2$-0.5 samples, with the total loading of NP and SiO$_2$ kept constant at 25 wt %.
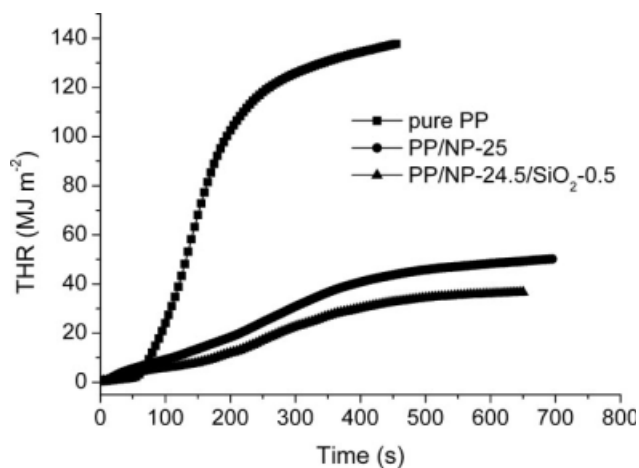

Figure 5 Dynamic curves of THR versus time for pure PP, PP/NP-25, and PP/NP-24.5/SiO$_2$-0.5 samples, with the total loading of NP and SiO$_2$ kept constant at 25 wt %.
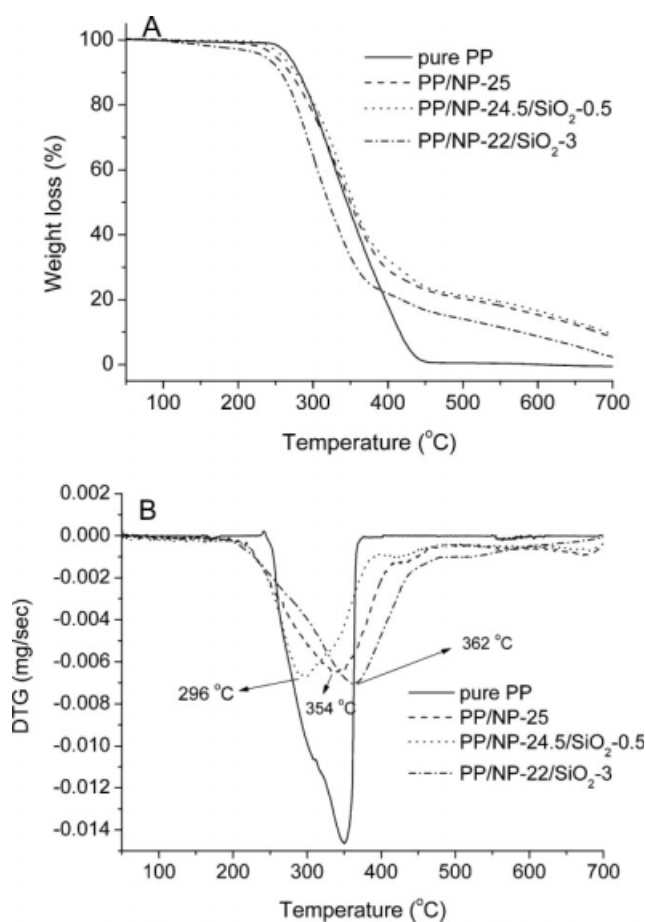
Figure 6 TGA (A) and DTG (B) curves of pure PP, PP/NP-25, and PP/NP-24.5/SiO$_2$-0.5 samples under a flow of air.

point of comparison, the thermal decomposition temperature 320°C of PP/NP-22/SiO$_2$-3 sample is 28 and 34°C lower than those of the PP/NP-25 (348°C) and PP/NP-24.5/SiO$_2$-0.5 (354°C) samples, respectively. The charred residues of PP/NP-25, PP/NP-24.5/SiO$_2$-0.5, and PP/NP-22/SiO$_2$-3 sample at 700°C are 8.9%, 10.1%, and 3.1%, respectively. It can be observed from Figure 6(B) that the maximum

mass loss peaks are observed at 290, 354, and 362°C for the PP/NP-22/SiO$_2$-3, PP/NP-25, and PP/NP-24.5/SiO$_2$-0.5 samples, respectively. It can be concluded that a suitable amount of fumed silica acting as a synergist with NP can enhance the thermal stability of PP/IFR blends, whereas excessive amounts of fumed silica will apparently decrease the thermal stability of PP/IFR blends.

Morphologic structures of charred layers from PP/IFR/SiO$_2$ blends

Figure 7 presents the SEM images of the intumescent charred layers from the PP/NP-25, PP/NP-24.5/SiO$_2$-0.5, and PP/NP-22/SiO$_2$-3 samples with the total loading of additives kept constant at 25 wt %. The charred layers of the PP/NP-25 sample are constituted of many closed cells, but the cells of charred layers were cracked, as shown in Figure 7(A). Therefore, the heat and flammable volatiles could penetrate the char layer into the flame zone during burning. However, the charred layers of the PP/NP-24.5/SiO$_2$-0.5 sample [Fig. 7(B)] show more compact and smoother structures without cracks than the PP/NP-25 sample, which could effectively limit the heat and mass transfer between polymer and flame. The charred layers of the PP/NP-22/SiO$_2$-3 sample show coarse and unshaped intumescent structures with holes. The fumed silica particles gathered on the surfaces can be clearly observed from Figure 7(C). The excessive amount of SiO$_2$ is easy to accumulate on the sample surface during the gasification/burning process because fumed silica has a large surface area and low density. When a suitable amount of fumed silica forms compact charred layers without cracking by collaborating with IFR, it acts as a heat insulation barrier. This kind of compact charred layer can prevent heat transfer and transportation of degraded products between melting polymer and surface and thus enhance the flame-retardant property.
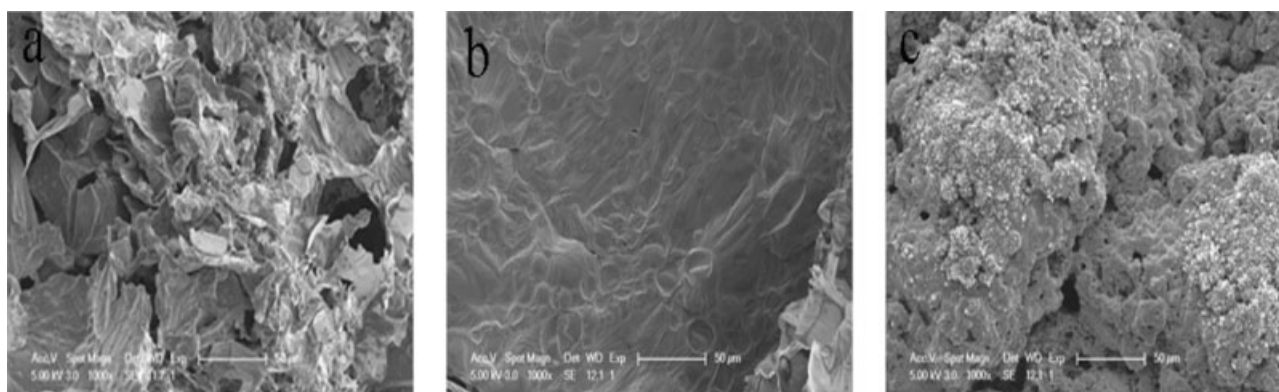

Figure 7 SEM images of the intumescent charred layers from PP/IFR blends with the total loading of NP and SiO$_2$ kept constant at 25 wt %. (A) PP/NP-25; (B) PP/NP-24.5/SiO$_2$-0.5; (C) PP/NP-22/SiO$_2$-3.0.
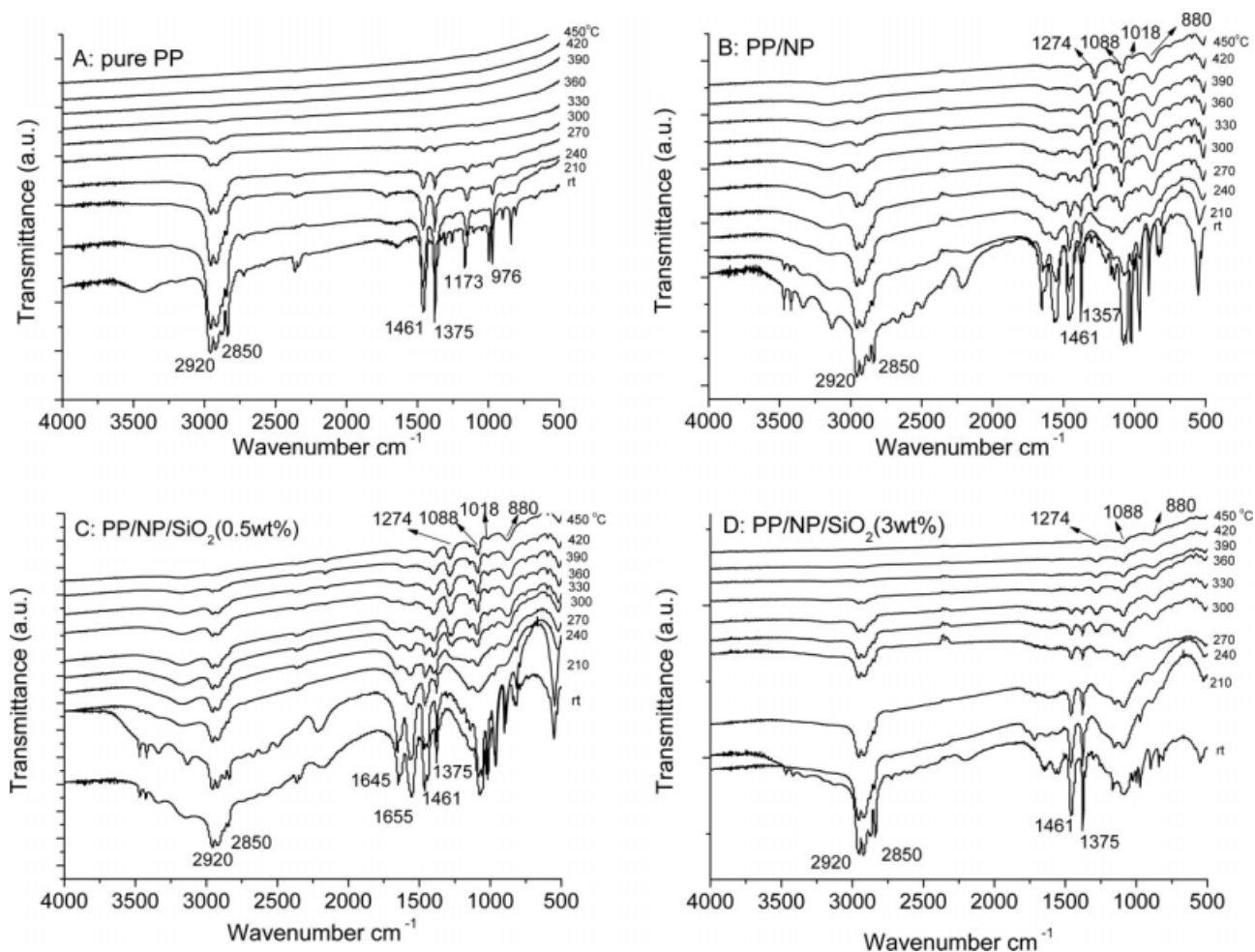
Figure 8 Dynamic FTIR spectra of various samples at different thermal-oxidative degradation temperatures: (A) pure PP; (B) PP/NP-25; (C) PP/NP-24.5/SiO₂-0.5; (D) PP/NP-22/SiO₂-3.

Dynamic FTIR spectra of PP/IFR/SiO₂ blends

Figure 8 shows the changes of dynamic FTIR spectra obtained from the thermo-oxidative degradation of pure PP, PP/NP-25, PP/NP-24.5/SiO₂-0.5, and PP/NP-22/SiO₂-3 samples with the total loading of NP and SiO₂ additives kept constant at 25 wt %. The detailed assignments of FTIR spectra in Figure 8 are presented in Table IV together with corresponding references.

The intensities of peaks at 2920, 2850 cm^{-1}, and 1461, 1375 cm^{-1} assigned to the asymmetric or symmetric vibration and deformation vibration of aliphatic group CH_2 or CH_3, respectively, decrease rapidly with increasing pyrolysis temperature. The disappearance temperatures of the aliphatic groups for the different samples were observed at 330°C for pure PP, 390°C for the PP/NP-25, 420°C for the PP/NP-24.5/SiO₂-0.5, and 360°C for PP/NP-22/SiO₂-3 samples, indicating that all the PP/IFR systems have higher thermal stability than pure PP. The PP/NP-24.5/SiO₂-0.5 sample has the highest thermal oxidation resistance.

The PP/IFR blends various peaks located at 800 to 1400 cm^{-1} can be observed in Figure 8(B), (C), and (D). The peak at 1274 cm^{-1} for the PP/NP-25 sample has been assigned to the stretching mode of P—O—C

TABLE IV
Assignments of Dynamic FTIR Absorption Peaks in Figure 8

| Wave number (cm^{-1})	Assignment	References
2,920	v_{as} of C—H in CH_2 or CH_3	16, 17
2,850	v_{sym} of C—H in CH_2 or CH_3	16, 17
1,700–1,800	C=O stretching vibration	5
1,461	γ-CH_2	17
1,375	γ-CH_3	17
1,350–1,360	Stretching mode in P=O	17
1,150–1,300	Stretching mode of P—O—C	17, 18
1,088	v_{sym} of P—O in P—O—P	4, 17
1,018	v_{sym} of PO_2 and PO_3 in phosphate-carbon complexes	17
976, 1,173	Vibration of CH_2—$CH(CH_3)$	19
880	v_{as} of P—O in P—O—P	5, 17
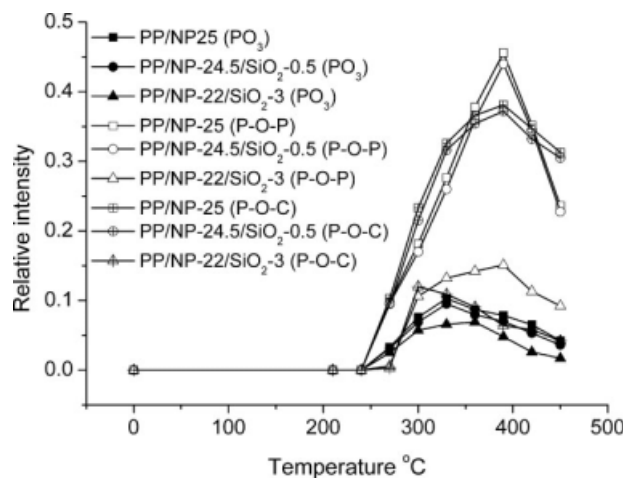
Figure 9 Relative peak intensities of various phosphoric acid derivatives at different thermal oxidative degradation temperatures obtained from Figure 8.

in the phosphocarbonaceous complex, the peaks at 1088 and 880 cm^{-1} assigned to the P—O vibration in P—O—P groups, and the peaks at 1018 cm^{-1} assigned to the symmetric vibration of PO$_3$ groups. Meanwhile, no new peaks can be found from the PP/NP-24.5/SiO$_2$-0.5 and PP/NP-22/SiO$_2$-3 samples by comparison with those of PP/NP-25 sample. All the above facts give positive evidence that the charred layers formed from the PP/NP blends consist of P—O—P, P—O—C, and PO$_3$ structural groups, and there is no effect of fumed silica on the chemical composition of charred layers, which means that the influence of SiO$_2$ is mainly due to its physical process in the condensed phase.

The formation rates of the P—O—C, P—O—P, and PO$_3$ products can be expressed by the change rates of relative peak intensities at 1274, 1088, and 1018 cm^{-1}, respectively. Figure 9 shows the changes of the relative intensities of P—O—C, P—O—P, and PO$_3$ products with the pyrolysis temperature for the PP/IFR systems. It is found from Figure 9 that the formation rates of the P—O—C, P—O—P, and PO$_3$ products in PP/NP-24.5/SiO$_2$-0.5 sample is a little lower than the PP/NP-25 sample. However, the formation rates of P—O—C, P—O—P, and PO$_3$ in the PP/NP-22/SiO$_2$-3 sample are much lower than those of the corresponding groups in the PP/NP-25 and PP/NP-24.5/SiO$_2$-0.5 systems when the pyrolysis temperatures increase to above 240°C. These results show that fumed silica restricts the formation of P—O—C, P—O—P, and PO$_3$ products in the charred layers. This is because the excessive amount of fumed silica with a large surface area accumulates easily on the surface, which obstructs the formation of intumescent charred layers. Only a suitable amount of fumed silica can act as a synergist with the NP additive to form compact charred layers and thus enhance the flame-retardant property of the PP/NP blends.

CONCLUSIONS

The synergistic effects of fumed silica on the PP/NP blends have been studied by FTIR spectroscopy, CCT, SEM, TGALOI, and UL-94 tests. The LOI and UL-94 data show that ≤1 wt % fumed silica apparently increases the LOI values and keep the V-0 rating. The CCT data indicate that a suitable amount of fumed silica can greatly reduce the HRR, MLR, and THR. The TGA curves show that only a suitable amount of fumed silica can increase the thermal stability of PP/IFR blends and leave more char residues after 500°C. The SEM and dynamic FTIR provide positive evidence that the flame-retardant synergistic effect of fumed silica with the IFR additive NP is due to the formation of compact charred layer and thus prevents the intumescent charred layer from cracking, which effectively protects the underlying polymer from burning. However, an excessive amount of fumed silica could restrict the formation of P—O—C, P—O—P, and PO$_3$ products in the charred layers and destroy the swelling behavior of intumescent charred layers, which would deteriorate the flame-retardant and thermal properties of the PP/IFR/SiO$_2$ blends.

References

1. Montezin, F.; Lopez-Cuesta, J.-M.; Crespy, A.; Georlette, P. Fire Mater 1997, 21, 245.
2. Halpern, Y.; Mott, D. M.; Niswarder, R. H. Ind Eng Chem Prod Res Dev 1984, 23, 233.
3. Hendrickson, L.; Connole, K. B. Polym Eng Sci 1995, 35, 211.
4. Xie, R. C.; Qu, B. J. Polym Degrad Stab 2001, 71, 375.
5. Xie, R. C.; Qu, B. J. Polym Degrad Stab 2001, 71, 395.
6. Wu, Q.; Qu, B. J. Polym Degrad Stab 2001, 74, 255.
7. Bourbigot, S.; Le Bras, M.; Delobel, R.; Breant, P.; Tremillon, J. M. Polym Degrad Stab 1996, 54, 275.
8. Liu, Y.; Wang, Q. Polym Degrad Stab 2006, 91, 2513.
9. Wang, D. Y.; Liu, Y.; Wang, Y. Z.; Perdomo, A. C.; Richard, H. T.; Dennis, P. Polym Degrad Stab 2007, 92, 1592.
10. Kashiwagi, T.; Gilman, J. M.; Butler, K. M.; Harris, R. H.; Shields, J. R.; Asano, A. Fire Mater 2000, 24, 277.
11. Fu, M. Z.; Qu, B. J. Polym Degrad Stab 2004, 85, 633.
12. Wickstrom, U.; Goransson, U. Heat Release in Fires; Babtauskas, V.; Grayson, S., Eds.; Elsevier: London, 1992; p 461.
13. Hirschler, M. M. Heat Release in Fire; Babrauskas, V.; Grayson, S., Eds.; Elsevier: London, 1992; p 375.
14. Qu, Y. Flame Retarded Polymeric Materials; National Defense Industry Press: Beijing, 2001.
15. Fontaine, G.; Bourbigot, S.; Duquesne, S. Polym Degrad Stab 2008, 93, 68.
16. Bourbigot, S.; Le, B. M.; Delobel, R. Carbon 1995, 33, 283.
17. Bugajny, M.; Bourbigot, S. Polym Int 1999, 48, 264.
18. Kwiatkowski, R.; Wlochowicz, A. J Mol Struct 2000, 516, 57.
19. Kranes, A.; Lange, A.; Ezrin, M. Plastics Analysis Guide; Hanser Publishers: New York, 1983.